Journal of Nuclear Materials 106 (1982) 211-220
North-Holland Publishing Company

INTERDIFFUSION AND CHEMICAL DIFFUSION IN THE UO_2 - $(U,Pu)O_2$ SYSTEM

D. Glasser-Leme*) and Hj. Matzke

Commission of the European Communities - Joint Research Centre
Karlsruhe Establishment - European Institute for Transuranium Elements
Postfach 2266 - D-7500 Karlsruhe

The chemical or interdiffusion of metal atoms (U and Pu) in the system $UO_{2\pm x}$-$(U,Pu)O_{2\pm x}$ was studied as function of oxygen potential, $\Delta\bar{G}(O_2)$ or O/M-ratio. High-resolution α-spectroscopy and electron microprobe analysis were used to measure diffusion profiles of couples of $UO_2/(U,Pu)O_2$ of different O/M-ratio. For most experiments, a mixed oxide of $(U_{0.83}Pu_{0.17})O_{2\pm x}$ was used. O/M-ratios were varied by using controlled mixtures of CO/CO_2. The Matano-Boltzmann-type analysis was employed to evaluate the interdiffusion curves. A pronounced dependence of the interdiffusion coefficients, $\tilde{D}$, on O/M-ratio was observed, with $\tilde{D}$ greatly increasing with increasing O/M-ratio. $\tilde{D}$ was also shown to increase with Pu-content in the range of about 4 to 17% Pu. Fast penetration of major quantities of Pu along grain boundaries into UO_2 was observed at high temperatures.

1. INTRODUCTION

Tracer self-diffusion in UO_2 and $(U,Pu)O_2$ has been studied in great detail (see e. g. (1,2)). In contrast, only comparatively little work has been done on interdiffusion in the system $UO_2 \cdot PuO_2$. Tracer metal atom diffusion depends strongly on oxygen partial pressure or O/M ratio (M=metal) and shows a minimum in rates at O/M$\sim$1.98 (T=1500°C). Such a composition is similar to the specified O/M for LMFBR fuels where substoichiometric compositions are used to minimize clad corrosion. At O/M$\sim$1.98, interdiffusion, formation of solid solutions and homogenization of mechanically blended UO_2 and PuO_2 powders during sintering and reactor operation are thus expected to be slow.

To obtain more data on interdiffusion, to study its dependence on O/M ratio and Pu-content and to find conditions for faster homogenization, the present study was started. Previous investigations of interdiffusion in the UO_2-$(U,Pu)O_2$ or UO_2-PuO_2 systems (3-6) or on homogenization of mechanically blended UO_2 and PuO_2 powders (7,8) had not selected the oxygen potential $\Delta\bar{G}(O_2)$ as controlled parameter. Also, the dependence of $\tilde{D}$ on Pu-content was not elaborated consistently. Rather, average values of $\tilde{D}$ were given in most cases.

The interdiffusion, hence the diffusion in the chemical gradient, is the basis of the homogenization process. The metal atom (U and Pu) mobility is rate-controlling since oxygen diffusion is much faster than the diffusion of U and Pu (e.g. (1)). Homogenization of UO_2-PuO_2 mechanical mixtures, or hence formation of solid solutions of $(U,Pu)O_2$, is interesting for a number of reasons, the most important being the solubility of the oxide in nitric acid. One of the other reasons was discussed at the last Conference on Characterization and Quality Control of Nuclear Fuels (9): During reduction, big voids can be formed in the remaining PuO_2 particles, probably due to build-up of water vapor originating from the reduction in hydrogen.

2. THE CHEMICAL OR INTERDIFFUSION COEFFICIENT, $\tilde{D}$

The chemical or interdiffusion coefficient, $\tilde{D}$, describes the mobility in a chemical gradient. If UO_2 and PuO_2 spe-

*) On leave from Instituto de Pesquisas Energéticas Nucleares, Sao Paulo, Brazil.

0022-3115/82/0000–0000/$02.75

cimens are facing one another, we obtain only one single $\tilde{D}$-value describing completely the resulting homogenization. In contrast, in pure UO_2, pure PuO_2, or in a solid solution of $(U,Pu)O_2$, hence in chemically homogeneous specimens and in the absence of a chemical gradient, metal transport is described by two (self)-diffusion coefficients, one for uranium and one for plutonium, D_U and D_{Pu}, the tracer diffusion coefficients. To relate D_U and D_{Pu} with $\tilde{D}$, the general solution developed by Cooper and Heasley (10) for binary ionic systems with 2 cations and a common anion can be used.

$$\tilde{D}=\left[\frac{Z_2N_{23}D_1(Z_3D_3-Z_2D_2)+Z_1N_{13}D_2(Z_3D_3-Z_1D_1)}{Z_1Z_3N_{13}D_3-Z_1^2N_{13}D_1+Z_2Z_3N_{23}D_3-Z_2^2N_{23}D_2}\right]\cdot$$

$$\cdot\left(1+\frac{d\ln a_{13}}{d\ln N_{13}}\right) \qquad (1)$$

where Z = valence, N = mole fraction, a = activity, and the subscripts 1 and 2 denote the cations and 3 the anion.

For UO_2 and PuO_2, $D_1 \sim D_2 << D_3$. With $Z_1=Z_2=4$, $Z_3=-2$, we obtain the Darken relation (11) (strictly valid for binary alloys)

$$\tilde{D} = (N_{UO_2}\cdot D_{Pu} + N_{PuO_2}D_U)\left(1+\frac{d\ln a_{UO_2}}{d\ln N_{UO_2}}\right) \qquad (1a)$$

Thus, for $N_{UO_2} \sim 0$, hence in nearly pure PuO_2, $\tilde{D} \simeq D_U$ and

for $N_{PuO_2} \sim 0$, hence in nearly pure UO_2, $\tilde{D} \simeq D_{Pu}$.

To measure $\tilde{D}$, the so-called MATANO-analysis is used (12). This yields different $\tilde{D}$-values along the curve of interpenetration U-Pu, hence we obtain the dependence of $\tilde{D}$ on the Pu-content (or U-content) of the oxide. For the details of the evaluation, the reader is referred to text-books (13).

For the system UO_2-PuO_2, an unusual difficulty exists that is not met in work with metals, alloys, or simple ionic materials such as CaF_2-BaF_2. This difficulty consists in the fact, that at most oxygen potentials of the annealing atmosphere, the valence of Pu is different from that of U, or hence the oxygen-to-metal ratio, O/M, is different in PuO_2, UO_2 and $(U_1\text{-}yPuy)O_2$. This is indicated in Fig. 1 where oxygen potential data for $(U_{0.8}Pu_{0.2})O_{2\pm x}$ and $UO_{2\pm x}$ for T=1500°C are plotted versus O/M-ratio.

The two arrows in the upper part of Fig. 1 indicate oxygen potentials used in this work. The difference in O/M-ratio between the two oxides can easily be of the order of 0.05.

The unavoidable consequence is shown in the lower part of Fig. 1. Since, at constant $\Delta\bar{G}(O_2)$, the valence v of Pu

$$v_{Pu} = 4 - 2x/y \qquad (2)$$

(where y = Pu-content, i.e. Pu/(U+Pu), or x = 0.5y $(4-v_{Pu})$) is constant, and therefore x depends on y, an O/M-gradient accompanies the Pu-profile that forms during interdiffusion.

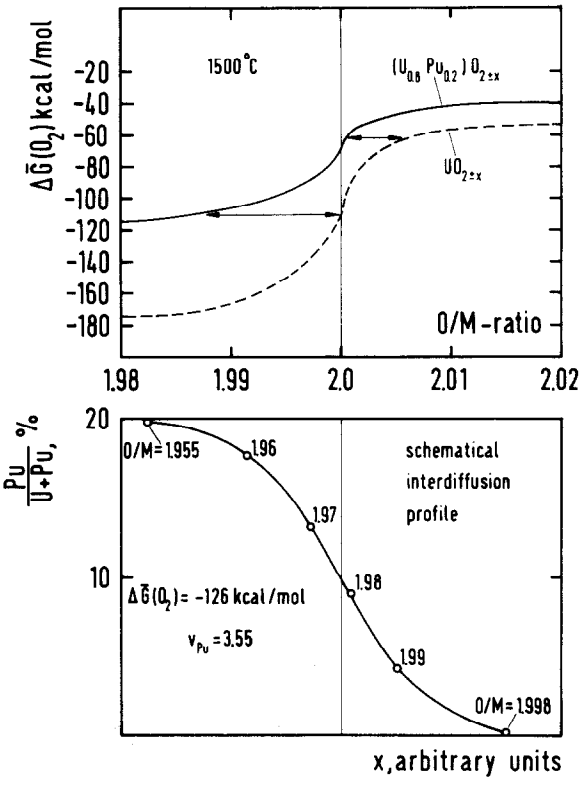

Fig. 1: Oxygen potential (average of published literature data) as function of O/M-ratio (upper part), and schematic interdiffusion profile (lower part). The O/M-gradient that forms along the Pu-gradient is indicated by circles with numbers representing the local O/M-ratios.

The existance of the O/M-gradient along the interdiffusion profile leads one to expect a strongly distorted profile. It

is known from tracer diffusion work (e. g. 2) that the tracer diffusion coefficients, D_U and D_{Pu}, vary strongly with O/M-ratio, as shown in Fig. 2 for D_{Pu} in $(U_{0.8}Pu_{0.2})O_2$.

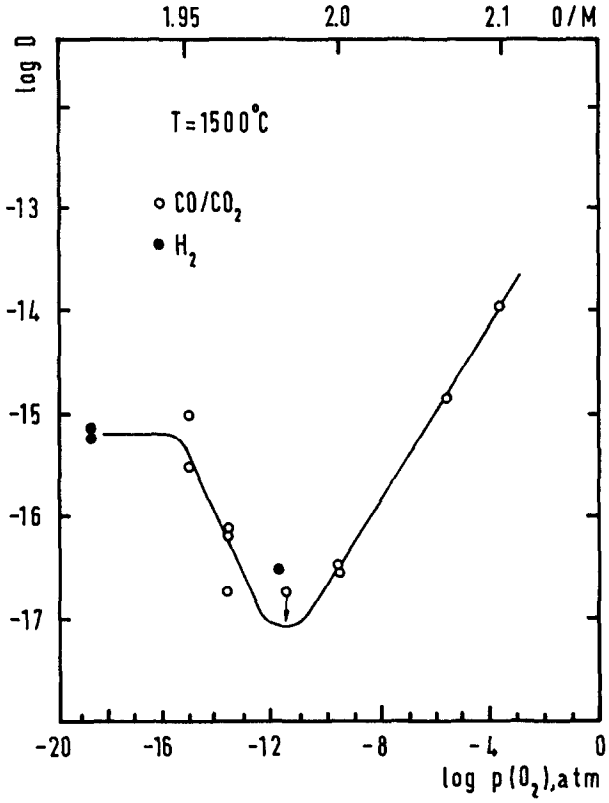

Fig. 2: Dependence of the tracer diffusion coefficient, D_{Pu}, on O/M-ratio in $(U_{0.8}Pu_{0.2})O_{2\pm x}$ for T=1500°C (2).

3. PREVIOUS WORK ON INTERDIFFUSION IN THE UO_2-PuO_2 SYSTEM

Table I lists the previous work on the topic of this study. Following the pioneering work of Theissen and Vollath (3), some in-pile investigations were published. During irradiation, the O/M-ratio of the fuel changes with burn-up and radial gradients in O/M-ratio develop. Also, chemical doping by in-growing fission products occurs, and the fission products redistribute radially along the existing temperature gradient. As a result, if $\tilde{D}$ is measured radially as function of T, as in the experiments of Butler and Meyer (5), a normal Arrhenius-type relation would not be expected to result, since different O/M-ratios and fission product concentrations would be expected at different temperatures. In the earlier work of Matzke (4), the dependence of $\tilde{D}$ on Pu-content was measured for the first time, but only at one temperature. As in refs. (3) and (5), average $\tilde{D}$-values were reported by Matzke and Lambert (14,15) from an investigation of gradients of U and Pu that form during incongruent evaporation. In this study, the O/M-ratio was controlled and used as a known parameter for the first time. Finally, the most recent investigation of Chilton and Edwards (6) attempted to study both the dependence of $\tilde{D}$ on Pu-content and O/M-ratio but the authors observed essentially only grain boundary penetration of Pu into UO_2. Results on other systems of the fluorite structure are summarized in Table II which is discussed below.

Table I: Previous Investigations on Interdiffusion in the System UO_2-PuO_2

Authors	year	ref.	method	T-range °C	$\frac{O}{M}$ - ratio	remarks
Theisen and Vollath	1967	3	empa	1450,1600	∿ 1.99	first pioneering work
Matzke	1971	4	α-radiography	2250	in-pile	1.5% burn-up,near-constant T and O/M
Butler and Meyer	1972	5	empa	1000-2000	in-pile	3,5 and 10% burn-up, radial profiles in O/M and fission products
Matzke and Lambert	1974/77	14,15	α-spectroscopy	1400-1800	1.9 -2.14	deduced from free incongruent evaporation
Chilton and Edwards	1978	6	empa	1750-1950	1.96-2.00	important grain boundary contribution

Table II: Comparison of results on interdiffusion in systems of the fluorite structure

System	CaF_2/SrF_2	SrF_2/BaF_2	CaF_2/YF_3	PuO_2/UO_2	CeO_2/UO_2	ZrO_2/HfO_2
ref.	17	18	19	this study	20	21
r_1/r_2 (4+)	0.89	0.84	-	0.96	0.95	1.01
(3+)	-	-	1.06	1.09	1.08	-
a_1/a_2	0.93	0.95	0.99	0.98	0.99	0.99
$\tilde{D}_o/\tilde{D}_{20}$ a)	2	3	40	20 - 200 b)	5 c)	~ 1

a) Change in $\tilde{D}$ for a change of one component of the diffusion couple of 0 to 20 mol %.

b) Increases with decreasing $\Delta\bar{G}(O_2)$, hence with increasing concentration of Pu^{3+}.

c) O/M-ratio (or concentration of Ce^{3+}) not known.

4. EXPERIMENTAL

Sintered pellets of UO_2 (density 94% of theor.) and of $(U_{0.83}Pu_{0.17})O_2$ (density 93% of theor.) were used. The average grain size was 8±1 µm. Results of chemical analyses are given in Table III.

O/M-ratios were established by annealing in a Pt/Rh-tube resistance furnace which did not contain any metallic parts in the annealing tube. 7 different gas mixtures of CO/CO_2 were used, corresponding to both oxidizing ($\Delta G(O_2)$ = -29.1 kcal/mol) or reducing conditions (-126.3 kcal/mol) (see Table IV).

Well polished faces of pellets of the two materials were placed together to form diffusion couples. No welding procedure was applied since work on tracer diffusion (e.g. 2) has shown the importance of following the time-dependence of diffusion at constant conditions (T, ΔG). This is only possible if the samples can be separated following different annealing steps. Table IV includes the duration of the diffusion anneals and the different steps (usually 3) that were used to follow the time-dependence of interdiffusion.

High resolution α-spectrometry and electron microprobe analysis (empa) were used to study the interdiffusion pro-

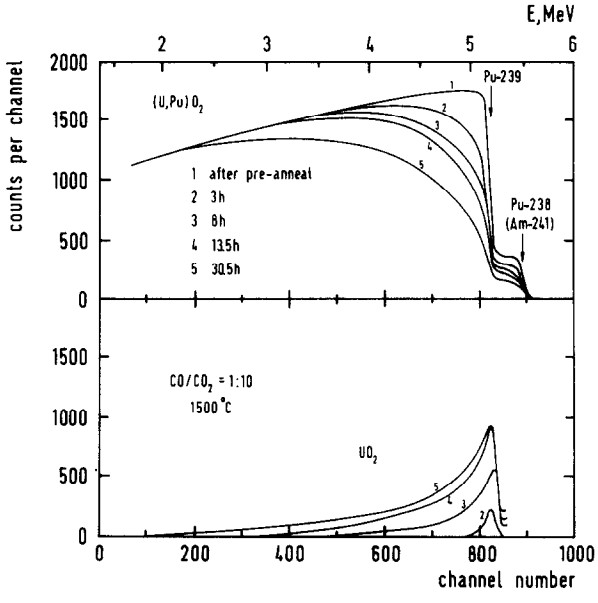

Fig. 3: Typical α-spectra of $(U,Pu)O_2$ and of UO_2 specimens before and following different steps of a diffusion experiment.

Table III: Analysis of impurities

Impurity	Concentration (ppm) in	
	UO_2	$(U_{0,83},Pu_{0,17})O_2$
Ag	0.19	< 0.2
Al	10	1000/300
B	0.22	1/0.5
Bi	1.99	< 1
Cd	< 0.46	
Cr	21	15
Cu	> 6.9	10/15
Fe	< 30	200/150
Mg	> 60	10/10
Mn	< 0.70	7/5
Mo	< 17	< 15
Na	17	
Ni	5	15/10
P		< 40
Pb	< 1.50	< 1
Si	73	50/30
Sn	0.85	< 1
V	< 0.48	< 15
W	< 70	
Zn	31	< 50

files. α-spectrometry was performed non-destructively on the surfaces of the two pellets of the diffusion couple. Empa was performed on sections cut perpendicular to the original surfaces, hence the specimens were destroyed and could only be used once.

5. RESULTS

Fig. 3 shows α-spectra of $(U,Pu)O_2$ and UO_2 before and following diffusion at constant temperature for 4 different annealing steps. The growing peak on UO_2 shows diffusion of Pu into UO_2. Only Pu is being measured with this technique. The $(U,Pu)O_2$ pellet shows two continua, a big one due to Pu-239 (maximum energy 5.15 MeV), and a smaller one due to a low percentage of short-lived (high specific activity) Pu-238 and Am-241 (both E_{max} = 5.50 MeV). The decreasing counting rate at the high energy end of the spectrum following the annealing steps shows progressive outdiffusion of Pu (or inwards diffusion of U) with increasing annealing time. The measured energy scale can be converted to the desired depth scale with the aid of measured energy loss values, dE/dx (22). The total range of the α-particles, hence the energy interval of 0 to 5.15 MeV, corresponds to a depth of 10.7 µm. The penetration curves established in this way were evaluated using the Matano-analysis.

Table IV: Experimental conditions for interdiffusion experiments

T = 1500 °C

Gas mixture CO : CO_2	$\Delta\bar{G}$ (O_2) kcal/mole	Annealing time, t h
1 : 10^2	- 29,1	10, 26, 66
1 : 10	- 45,3	8, 14, 31
1 : 1	- 61,3	24, 66
10 : 1	- 77,7	23, 47, 130
10^2 : 1	- 93,9	33, 67, 131
10^3 : 1	- 110,1	37, 103, 169
10^4 : 1	- 126,3	35, 54, 118

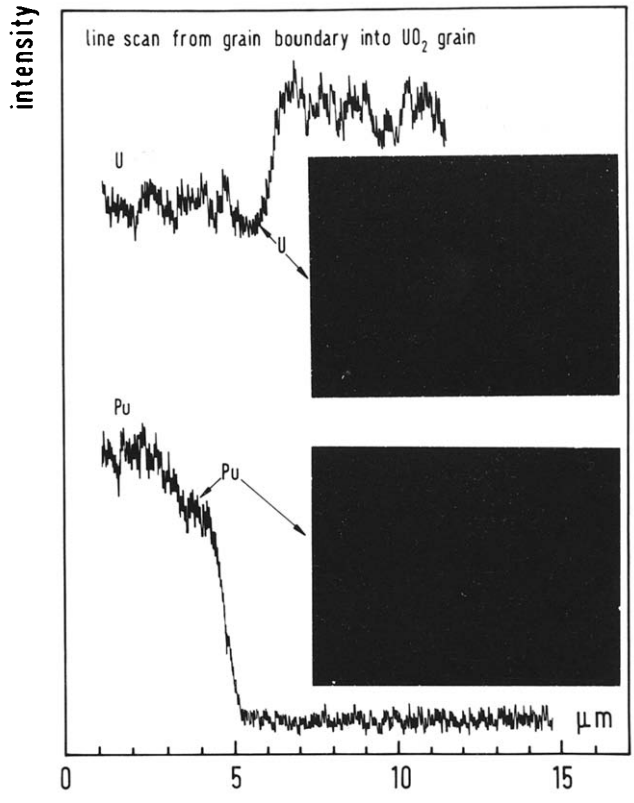

Fig. 4: Typical empa result for an anneal at T=1925 °C. Grain boundary penetration of Pu into UO_2 is seen whereas the diffusion profiles into the UO_2 grains are very steep.

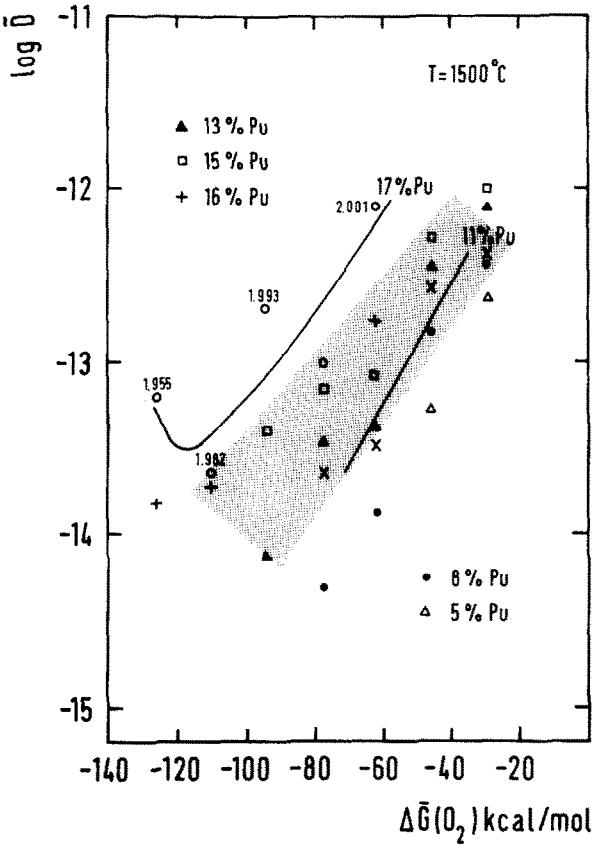

Fig. 5: The interdiffusion coefficient, $\tilde{D}$, for the system UO_2-PuO_2, for T=1500°C, as function of oxygen potential, $\Delta\bar{G}(O_2)$, with Pu-content (or depth in $(U,Pu)O_2$) as parameter.

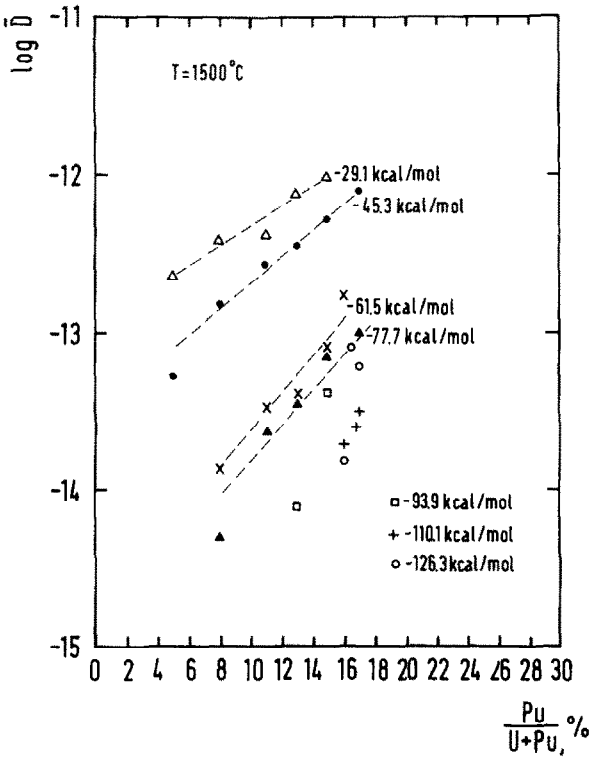

Fig. 6: The interdiffusion coefficient, $\tilde{D}$, for the system UO_2-PuO_2, for T=1500°C, as function of Pu-content (or depth in $(U,Pu)O_2$), with $\Delta\bar{G}(O_2)$ as parameter.

Fig. 4 shows typical empa results. The X-ray scanning pictures demonstrate deep penetration of Pu all around the UO_2 grains. In contrast, the line scan from a grain boundary into a UO_2 grain shows very steep profiles for both U and Pu indicating that interdiffusion within the lattice is very slow compared with grain boundary penetration.

Figs. 5 and 6 show a first evaluation of the Matano-analysis obtained by α-spectrometry. The same data for $\tilde{D}$ are plotted once versus $\Delta\bar{G}(O_2)$, or O/M-ratio, with the Pu-content being parameter, and once versus Pu-content, with the oxygen potential, $\Delta\bar{G}(O_2)$ being parameter.

Figs. 5 and 6 demonstrate a very pronounced effect of the oxygen potential of the annealing atmosphere. At constant Pu-content, $\tilde{D}$ increases by up to 2 orders of magnitude, if $\Delta\bar{G}(O_2)$ increases from reducing conditions (e.g.-120 kcal/mol) to oxidizing conditions (e.g.-30 kcal/mol). The dotted area in Fig. 5 indicates this trend. Whether or not a minimum exists as in tracer diffusion (see Fig. 2) is not clear yet. More results at lower oxygen potential would be needed. A minimum is tentatively indicated in Fig. 5 for a Pu-content of 17% (see full line). The small numbers next to the data points show the corresponding O/M-ratios. The possibly indicated minimum would also be at O/M≈1.98, as in tracer diffusion.

There is also a dependence of $\tilde{D}$ on Pu-content which, however, is less pronounced than that on $\Delta\bar{G}(O_2)$, at least in the range of Pu-contents studied. It is more pronounced at lower $\Delta\bar{G}(O_2)$, hence under reducing conditions where an increasing amount of Pu is trivalent. This dependence of $\tilde{D}$ on Pu-content may, however, also be influenced by grain boundary effects as those shown in Fig. 4. This will be discussed below.

6. DISCUSSION

The present study reports interdiffusion coefficients $\tilde{D}$ for the system UO_2-PuO_2 for controlled and constant oxygen potential. Most previous publications had given average $\tilde{D}$-values, whereas in this study, the dependence of $\tilde{D}$ on Pu-content was also systematically investigated. So far, systematic data were obtained for one temperature only, i.e. T=1500°C, though in total the temperature range between 1300 and 2200°C was covered. These data will be reported later.

A pronounced effect of oxygen potential or O/M-ratio on $\tilde{D}$ was found. Such an effect was expected, based on tracer diffusion measurements of U and Pu in $(U,Pu)O_{2\pm x}$ and $UO_{2\pm x}$ (e.g. 1, 2). For tracer diffusion, the O/M-ratio was concluded to be important in determining D_U and D_{Pu} whereas the valence state (Pu^{3+} or Pu^{4+}, U^{4+} or U^{5+} and U^{6+}) was said to be less important. A point defect model (2) was used to explain the data as those shown in Fig. 2. Metal vacancies, the concentration of which increases with x in MO_{2+x}, provide fast mobilities in oxidized specimens. With decreasing x, the metal vacancy concentration decreases until, at O/M below 1.98 (for T=1500°C), metal interstitials dominate. The minimum at O/M≈1.98 for T=1500°C is expected to depend on temperature. It would be expected to be at smaller O/M-ratios at higher temperatures. Below O/M≈1.95 at T=1500°C, finally, formation of clusters between two Pu^{3+} ions and an oxygen vacancy, etc. were said to explain the constant D-values at O/M<1.95 (2). As shown in equs. (1) and (1a), $D \propto D_U$ and D_{Pu}. The strong decrease of the tracer values D_U and D_{Pu} with decreasing x would thus be expected to be reflected in $\tilde{D}$.

Values for the thermodynamic factor $d\ln a_{UO_2}/d\ln N_{UO_2}$ have not been published so far, to the authors' knowledge. Within the Transuranium Institute, oxygen potential measurements on $(U,Pu)O_{2\pm x}$ are being performed which are hoped to yield reliable information on this factor. This would allow to perform a theoretical prediction of $\tilde{D}$, as could be done for oxygen diffusion in UO_2 and $UO_{2\pm}$ (e.g. 23,24). Without this information, a comparison with data for other systems might be used to understand the present results on the dependence of $\tilde{D}$ on Pu-content. Table II summarizes the interdiffusion results on related systems of the fluorite structure. The variation of $\tilde{D}$ with the concentration of the cations, expressed as ratio of D_0 (e.g. pure CaF_2) and of D_{20} (e.g. $Ca_{0.8}Sr_{0.2}F_2$), is smallest for the system ZrO_2/HfO_2, where both cations have the same valence and very similar ionic radii, r, (1% difference) and where the lattice constants, a, of the pure compounds are very similar (again 1% difference). At still identical valence but increasing differences in lattice constants, a, and ionic radii, r, the variation of $\tilde{D}$ with cation concentration increases (cases CaF_2/SrF_2 and SrF_2/BaF_2). With the possibility of different valences (CeO_2/UO_2, where Ce can be 3+ or 4+), a further increase is seen. Whenever the valences are definitely different (Y^{3+} and Ca^{2+}), the variation becomes important. The present study reports an even more pronounced dependence. This dependence increases with increasing differences in r, i.e. with increasing reduction of the oxide.

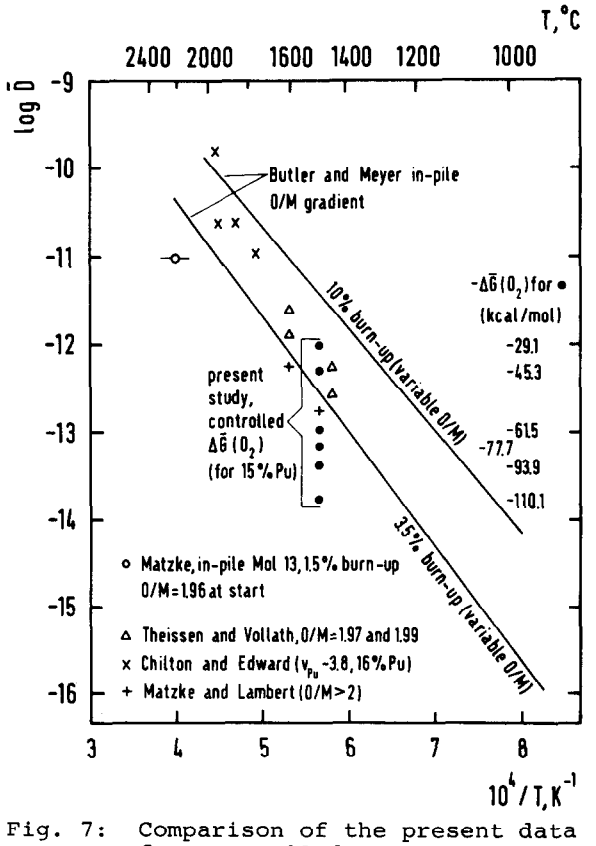

Fig. 7: Comparison of the present data for controlled oxygen potential, with literature data published previously. An Arrhenius diagram is used for this comparison as convenient but strictly inadequate presentation.

Two words of caution should, however, be added: First, as shown in Fig. 1, the influences of O/M-ratio and of Pu-content

cannot easily be separated. The reason is the varying O/M-ratio, despite of the constant and controlled $\Delta\bar{G}(O_2)$, along the Pu-profile. Second, the highest $\tilde{D}$-values are calculated for the highest Pu-content, i.e. for the most deeply extending part of the profile. As shown in Fig. 4, grain boundary penetration is important, and these values are therefore expected to be high due to grain boundary contributions. Future experiments with single crystals will allow to correct for this source of error.

A pronounced grain boundary penetration was also reported by Chilton and Edwards (6). It is even known from work with metals (25) that a first step of homogenization can be enveloping of one type of particles by a layer of the other substance, before true interdiffusion within the lattice becomes important. The enveloping of UO_2 by PuO_2, its reason and its quantitative effect on homogenization, interdiffusion and formation of solid solutions need further investigation.

The present data are compared with literature results (see Table I) in Fig. 7. An Arrhenius-type presentation was selected though this is strictly not a valid procedure for most data. For instance, the results of Butler and Meyer (5) are given by two lines, taken from the corresponding figures of these authors. These results were obtained within operating fuel elements where a pronounced temperature gradient exists with important radial redistributions of U,Pu, fission products and, very importantly, of oxygen. Such data are thus not only average $\tilde{D}$-values, but they probably also represent different O/M-ratios, doping levels etc. along the temperature gradient. Strictly, a straight line in an Arrhenius diagram for interdiffusion is only valid for constant O/M-ratio and (not or) constant Pu-valence with, simultaneously, constant Pu-content.

The most noteworthy point in comparing the present data with the previous ones is the fact, that only the high results for oxidized specimens are comparable with most previous data whereas the new results for reducing conditions are lower than most literature data. This might indicate that fast grain boundary penetration affected many of the previous results.

7. CONCLUSIONS AND SUMMARY

The present study, performed on sintered UO_2 and $(U_{0.83}Pu_{0.17})O_2$, shows a pronounced dependence of the interdiffusion coefficient, $\tilde{D}$, on O/M-ratio. 7 different gas mixtures of CO/CO_2 were used to guarantee constant and known oxygen potentials. Following preliminary experiments in a wide temperature range of 1300 to 2200°C, systematic measurements were made at T=1500°C.

The interdiffusion rates depended also on the Pu-content of the oxide. Very low rates were observed in reduced oxides (O/M$\sim$1.98). Such compositions correspond to the specifications of fast breeder elements. Much higher rates (by a factor of $\sim 10^2$) of interdiffusion were observed under slightly oxidizing conditions. Much faster homogenization and formation of solid solution would be expected under these conditions as well.

Future systematic experiments will be performed at lower oxygen potentials, higher temperatures and higher Pu-contents. Single crystals will be used to fully understand the effect of fast penetration of Pu along grain boundaries.

The present data show that any calculational or theoretical treatment of homogenization of mechanically mixed UO_2-PuO_2 should not use tracer D-values as was done so far, but should rather use $\tilde{D}$-values and allow for their dependence on Pu-content and O/M-ratio, except in the cold outer part of the fuel where it is suggested that $D \sim D$ (tracer) = D^*, the radiation enhanced diffusion coefficient. The athermal, hence temperature independent value of

$$D^* = 1.2 \times 10^{-29} \dot{F} \quad cm^2 s^{-1},$$

with $\dot{F}$ = fission rate in f $cm^{-3} s^{-1}$ as reported before (26,27) is suggested for this part of the fuel, largely independent of composition.

ACKNOWLEDGEMENTS

The authors would like to thank K.Richter for providing the sintered pellets and C.Walker for performing empa investigations. Thanks are also due to V. Meyritz and G.Zeibig for experimental help.

REFERENCES

1) Hj. Matzke, in Plutonium 1975 and other Actinides, North Holland Publ. Comp., (1976) p. 801

2) Hj. Matzke, in Proc.Int.Conf. on Transport in Nonstoichiometric Compounds, Cracow, Poland, Ed. J. Nowotny, North Holland Publ. Comp., in print (1981)

3) R. Theisen and D. Vollath, in Plutonium as a Reactor Fuel, IEAE (Vienna), (1967) p. 253

4) Hj. Matzke, Progress Report TUSR-11, (1973) 21

5) E.M. Butler and R.O. Meyer, J. Nucl. Mater. 47 (1973) 229

6) G.R. Chilton and J. Edwards, J. Nucl. Mater. 78 (1978) 182

7) R. Verma, J. Nucl. Mater. 80 (1979) 43

8) H. Furuya, H. Tajiri and M. Koizumi, this Conference, J. Nucl. Mater.

9) M.D. Freshley, D.W. Brite, J.L. Daniel and P.E. Hart, J. Nucl. Mater. 81 (1979) 63

10) A.R. Cooper, Jr. and J.H. Heasley, J. Amer. Ceram. Soc. 49 (1966) 280

11) L.S. Darken, Trans. AIME 175 (1948) 184

12) C. Matano, Japan. Phys. 8 (1933) 109

13) P.G. Shewmon, Diffusion in Solids, McGraw-Hill, N.Y. (1963)

14) Hj. Matzke and R.A. Lambert, J. Nucl. Mater. 49 (1974) 325

15) Hj. Matzke and R.A. Lambert, J. Nucl. Mater. 64 (1977) 211

16) M. Bober, G. Schumacher and D. Geithoff, J. Nucl. Mater. 47 (1973) 187

17) R.W. Scheidecker and M.F. Berard, J. Amer. Ceram. Soc. 56 (1973) 204

18) R.W. Scheidecker and M.F. Berard, J. Amer. Ceram. Soc. 59 (1976) 431

19) R.G. Visser, W.F. Schiavi and M.F. Berard, J. Amer. Ceram. Soc. 58 (1975) 438

20) P. Jean-Baptiste, PhD-Thesis, Université de Paris-Sud, Centre d'Orsay (1980)

21) Y. Oishi, Y. Sakka and K. Ando, J. Nucl. Mater. 96 (1981) 23

22) V. Nitzki and Hj. Matzke, Phys. Rev. B8 (1973) 1894

23) W. Breitung, J. Nucl. Mater. 74 (1978) 10

24) Hj. Matzke, Proc. Int. Conf. Fast Breeder Reactor Fuel Performance, Monterey (1979) Am. Nucl. Soc., Cat. No. 79-50775

25) B. Fisher and P.S. Rudman, J. Appl. Phys. 32 (1961) 1604

26) A. Höh and Hj. Matzke, J. Nucl. Mater. 48 (1973) 157

27) Hj. Matzke, Europ. Appl. Research Reports - Nucl. Sci. Techn. 1 (1979) 287, also Report EUR-6600 EN

DISCUSSION

K. Kummerer (KfK Karlsruhe, Germany)

Since with an enhanced O_2 offer the interdiffusion greatly increases, I ask the following question to the manufacturers of mixed oxide: Would it not be possible to influence in a favorable way the solubility of mixed oxide by providing sintering conditions involving a higher O_2 offer ?

H. Roepenack (ALKEM Hanau, Germany)

Attempts in this direction were undertaken. Although they improved the solubility they had not been sufficient to meet the specified requirement. Since the other techniques allowed to attain the goal at a faster rate and under safer conditions, the said experiments were discontinued.

D. Hanus (ALKEM Hanau, Germany)

Besides the unsatisfactory results of solubility for hyperstoichiometric sintering large variations in the sintering density are obatined at sintering temperatures > 1700 K. Under the conditions stated, both effects rule out a fabrication technique.

H. Bairiot (Belgonucléaire Brussels, Belgium)
Our experience indicates that the sintering under controlled O-potential conditions influences also the microstructure. While this may be applicable to small diameter pellets, our experience with large diameter BWR pellets leads to the conclusion that the gradients of O-potential across the pellet diameter influences the microstructure in a non-controllable manner under conditions of industrial manufacturing.